Journal of Engineering Mathematics, Vol. 15, No. 2, April 1981

Leading-edge separation from a thick, conical, slender wing at small angless of incidence

J. NUTTER*

School of Mathematics and Physics, University of East Anglia, Norwich, U.K.

(Received August 5, 1980)

SUMMARY

The inviscid separated flow past slender rhombic cones at incidence is considered. A complex potential is constructed, in a suitable cross-flow plane, which satisfies the conditions on the wing, at infinity, and on the vortex system which models the separated flow. The results obtained both extend earlier results to small incidence, and explain an anomaly within those results.

1. Introduction

In this paper we consider the symmetric flow past slender wings, in the form of rhombic cones, at incidence. We model the separation from the leading edge by spiral vortex sheets in an inviscid, potential-flow model. The vortex sheets are infinite in extent and in our treatment we replace the spiral by a finite sheet springing from the leading edge, and model the inner part of the sheet by an isolated vortex core, which is joined to the end of the sheet by a cut. This model of a separated flow was first used by Smith [1] in his study of the flow past a slender delta wing at incidence. These results were subsequently extended by Barsby [2] to include the effect of blowing from the leading edges, and [3] to very low incidences. Meanwhile Smith [4] used the model in his study of the flow past slender rhombic cones and the present work is an extension of [4].

The use of slender-body theory reduces the problem under consideration to the solution of Laplace's equation in the cross-flow plane. The first step is the conformal transformation of the wing, via a Schwarz-Christoffel transformation, into a section of the imaginary axis in the transformed plane. The wing boundary condition is satisfied by a distribution of sources on the transformed contour. The complex velocity which satisfies the conditions on the wing and at large distances from it is readily available. It includes the vortex sheets and isolated vortices whose positions and strengths are unknown. These are determined from the conditions that the vortex sheets coincide with stream surfaces and that across them there is no jump in pressure, together with a condition that the overall force on the isolated vortex and cut is zero, and that the velocity is finite at the leading edge. The discretization of the sheet boundary conditions reduces the problem to the solution of a set of nonlinear algebraic equations.

* Present address: Hunter Douglas Europe, Rotterdam, The Netherlands

Our treatment of the problem differs from that in [4] in two distinct ways. The first and most important difference is associated with the treatment of the source-integral which accommodates the wing boundary condition. The treatment in [4] effectively replaces the continuous source distribution by a set of discrete sources, and this leads to anomalous results as a suitably defined incidence parameter decreases. In Section 3 below we show, using the results of an Appendix in [4], how the source-integral may be evaluated analytically and so enable us to extend the results of [4] as the incidence parameter decreases. A second difference concerns the iterative procedure employed to solve the nonlinear algebraic equations. Thus the nested iterative scheme of [4] is replaced by a direct Newton iteration scheme which is fully described in [5]. This provides rapid convergence to a solution vector from a starting value appropriate to a neighbouring solution in the two-parameter space with which we work.

The results which we have obtained show the effect of wing thickness upon the vortex configuration and the circulation about it. In particular we demonstrate that for a wing of given thickness the vortex system collapses into the leading edge of the wing as the incidence tends to zero, and we thus remove the anomaly associated with the results of [4].

2. Formulation of the problem

With reference to Fig. 1 we consider, in the slender body and conical flow approximations, the flow past a thick delta wing in the form of a rhombic cone. With origin O at the wing apex the x-axis forms the centre-line of the wing with the y, z-axes in the plane of the cross section of the wing. The undisturbed stream of speed U makes an angle α with the x-axis, and the angle between the wing centre line and the leading edge is γ.

At a distance x from O the wing has a rhombic cross section, of semi-span $s = Kx$ where $K = \tan\gamma$, and the angle between the wing surfaces at the leading edge is δ. It proves convenient to define

$$\epsilon = (\pi - \delta)/2\pi, \tag{2.1}$$

so that $\epsilon\pi$ is the angle shown in Fig. 1.

Following Smith [4] we adapt the slender-body theory of Ward [6] to our present problem. Thus, in the slender-body approximation, we write the complete velocity potential as

$$U\{x + b_0(x)\} + \Phi \tag{2.2}$$

where Φ is a harmonic function of y and z. If M denotes the free-stream Mach number and $S(x)$ the local cross-sectional area of the wing, then $b_0(x)$ in (2.2) is defined from

$$2\pi b_0(x) = S'(x)\ln\frac{1}{2}\beta + \frac{1}{2}\int_x^1 S''(t)\ln(t-x)\,dt - \frac{1}{2}\int_0^x S''(t)\ln(x-t)\,dt,$$

where $\beta^2 = 1 - M^2$ for subsonic speeds, and

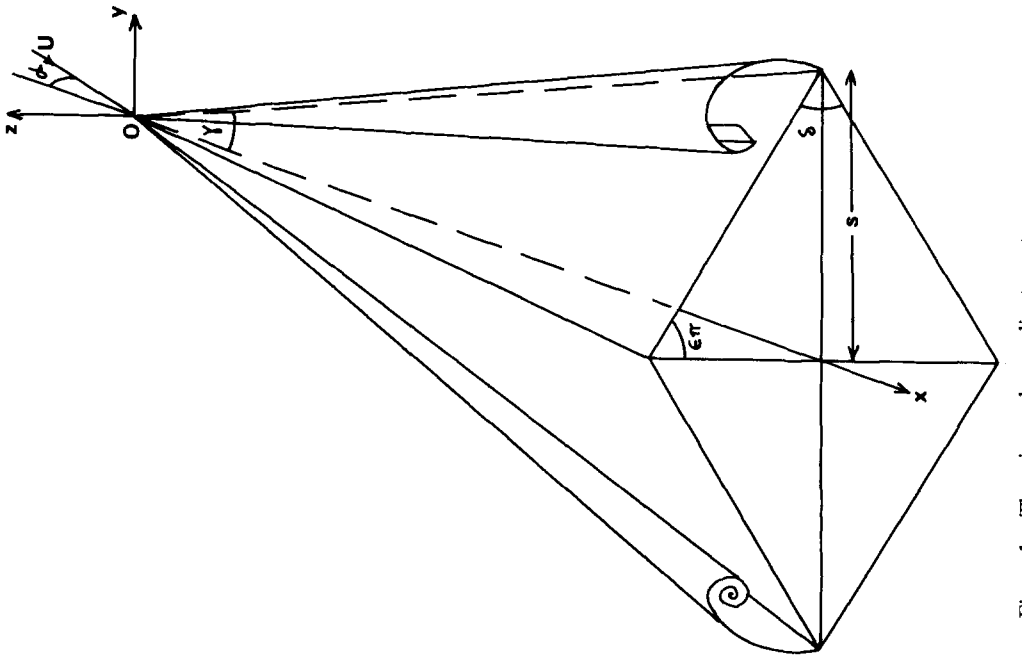

Figure 1. The wing and co-ordinate system.

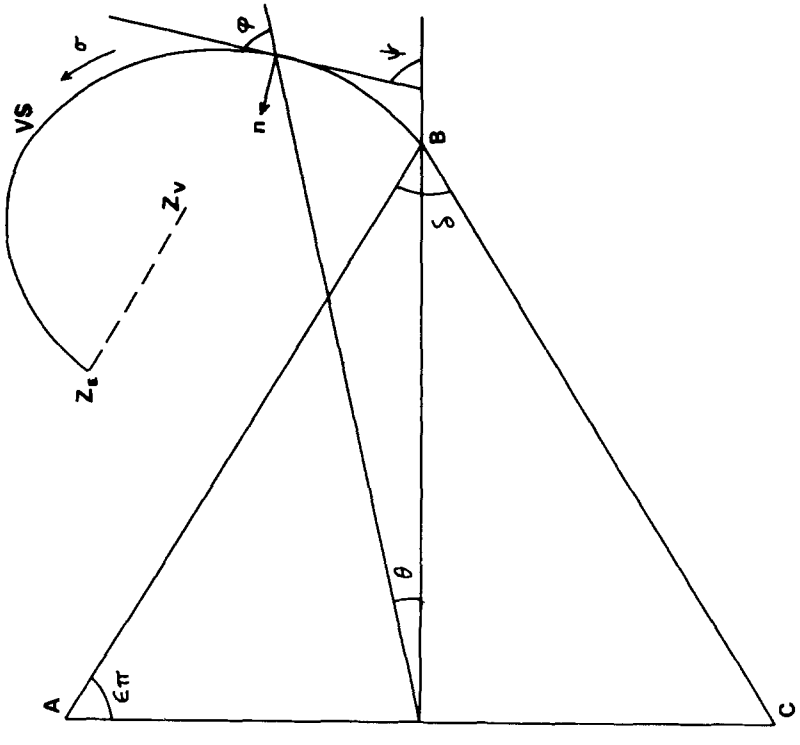

Figure 2. The cross-flow plane. The vortex sheet is denoted by VS, the cut is represented thus – – – – –.

$$2\pi b_0(x) = S'(x) \ln \frac{1}{2} B - \int_0^x S''(t) \ln (x - t)\, dt,$$

with $B^2 = M^2 - 1$ for supersonic speeds. The problem then reduces to solving

$$\Phi_{yy} + \Phi_{zz} = 0, \tag{2.3}$$

with

$$\frac{\Phi}{U} \sim \alpha z + \frac{S'(x)}{2\pi} \ln r \tag{2.4}$$

at large distances from the wing, where $r^2 = y^2 + z^2$, together with other boundary conditions on the wing and vortex sheets. For present purposes there is no need to consider $b_0(x)$ further.

Before introducing other boundary conditions it is convenient to define dimensionless variables as

$$x' = \frac{Kx}{s}, \quad y' = \frac{y}{s}, \quad z' = \frac{z}{s}, \quad r' = \frac{r}{s}, \quad \phi = \frac{\Phi}{KUs}. \tag{2.5}$$

We now consider the boundary conditions, following Smith [1], [4], for ϕ which supplement (2.4). First we consider the boundary conditions on the vortex sheets which spring from the leading edges as shown in Fig. 1. Thus the condition that the vortex sheet is a stream surface gives (the primes on independent variables are henceforth omitted)

$$\phi_n = -r \sin \varphi, \tag{2.6}$$

where **n** is the inward normal, and φ the angle between the tangent and radius vector as shown in Fig. 2. The condition that there is no pressure difference across the vortex sheet may be represented as

$$\Delta\phi = \Delta\phi_\sigma (r \cos\varphi - \phi_{\sigma_m}), \tag{2.7}$$

where Δ is the difference operator across the sheet (inside minus outside), σ is arc length along the cross-section of the sheet as in Fig. 2, and the suffix m denotes the mean value across the sheet. The boundary condition on the wing surface, where $r \sin\varphi = \cos \epsilon\pi$, follows from (2.6) as

$$\phi_n = -\cos \epsilon\pi. \tag{2.8}$$

Finally, at the leading edge of the wing where separation takes place, we impose the Kutta condition that the velocity is finite.

Following Smith [1], [4], we do not attempt to satisfy the conditions (2.6), (2.7) at all points of the vortex sheet, which is infinite in extent. Thus we represent the vortex sheet by a finite part springing from the leading edge and an isolated line vortex, as shown on the starboard half-wing in Fig. 1. The inner part of the sheet beyond E is concentrated into the line vortex at V; across the cut which is left behind the velocity potential jumps by an amount equal to the circulation about the line vortex. Equation (2.7) cannot be satisfied at the cut and we replace it

by the condition that the total force on vortex and cut be zero. If $W(Z)$ is the complex potential , such that $\phi = \mathrm{Re}(W)$, with the complex variable $Z = y + iz$, then this condition of zero total force may be written as

$$\lim_{Z \to Z_V} \left(\frac{\mathrm{d}W}{\mathrm{d}Z} - \frac{\Gamma}{2\pi i} \frac{1}{Z - Z_V} \right) = 2\bar{Z}_V - \bar{Z}_E, \tag{2.9}$$

where Γ is the circulation of the starboard isolated vortex, Z_V, Z_E represent the positions of the isolated vortex and end of the cut respectively, and an overbar denotes the complex conjugate.

To construct the complex potential it is convenient, as in [4], to first introduce a conformal transformation in which the region of the Z-plane to the right of the wing and the imaginary axis transforms into the half-plane $\mathrm{Re}(Z^*) > 0$. Thus we write

$$Z = 1 + \int_0^{Z^*} \left(\frac{t^2}{t^2 + d^2} \right)^{\epsilon} \mathrm{d}t, \tag{2.10}$$

and we note that the points A and C on the wing centre-line transform to $Z^* = \pm id$, whilst the leading edge B transforms to the origin $Z^* = 0$. The Z^*-plane is shown in Fig. 3.

The wing boundary condition is accommodated by the introduction of a source distribution along the slit ABC in the transformed plane of strength

$$2 \cos \epsilon\pi \left| \frac{\mathrm{d}Z}{\mathrm{d}Z^*} \right| \tag{2.11}$$

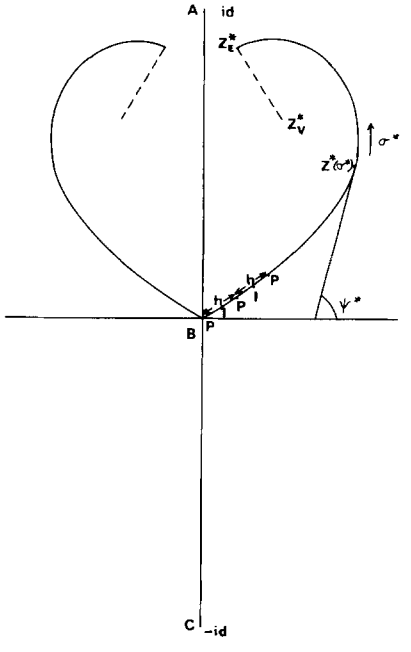

Figure 3. The transformed plane. The pivotal and intermediate points are denoted by P and I respectively.

per unit length, as required to produce the normal velocity $\cos \epsilon\pi \left| \mathrm{d}Z/\mathrm{d}Z^* \right|$ directed outwards from the slit ABC. It can be shown [4], reverting to dimensional form, that the total source strength is $US'(x)$ and as a consequence the sources account for the logarithmic behaviour of Φ, at large distances, shown in (2.4). The remaining term in (2.4) is accounted for by a uniform stream parallel to the imaginary axis in the Z^*-plane. The complex velocity for the attached flow in the Z^*-plane can therefore be written as

$$-ia + \frac{\cos \epsilon\pi}{\pi i} \int_{-id}^{id} \left| \left(\frac{t^2}{t^2 + d^2} \right)^{\epsilon} \right| \frac{\mathrm{d}t}{Z^* - t}, \tag{2.12}$$

where $a = \alpha/k$ is the incidence parameter. The velocity field is completed by the addition of contributions from the vortex system, thus

$$\frac{\mathrm{d}W}{\mathrm{d}Z^*} = -ia + \frac{\cos \epsilon\pi}{\pi i} \int_{-id}^{id} \left| \left(\frac{t^2}{t^2 + d^2} \right)^{\epsilon} \right| \frac{\mathrm{d}t}{Z^* - t} +$$

$$+ \frac{\Gamma}{2\pi i} \left(\frac{1}{Z^* - Z_V^*} - \frac{1}{Z^* + \bar{Z}_V^*} \right) + \frac{1}{2\pi i} \int_0^{\sigma^*_{\max}} g^*(\sigma^*) \left(\frac{1}{Z^* - Z^*(\sigma^*)} - \frac{1}{Z^* + \bar{Z}^*(\sigma^*)} \right) \mathrm{d}\sigma^*, \tag{2.13}$$

where $\sigma^*_{\max}$ is the arc length of the vortex sheet from the origin to Z_E^* and $g^*(\sigma^*)$ denotes the sheet strength in the transformed plane and is given by

$$g^*(\sigma^*) = -\frac{\mathrm{d}\Delta\phi}{\mathrm{d}\sigma^*}. \tag{2.14}$$

Equation (2.13) defines a complex potential W which correctly satisfies the condition (2.8) at the wing surface, and the condition (2.4) at infinity. For it to represent a solution of our problem the position Z_V^* and strength Γ of the isolated vortex, together with the position $Z^*(\sigma^*)$ and strength $g^*(\sigma^*)$ of the vortex sheet must be determined from the conditions (2.6), (2.7), (2.9) and the Kutta condition of finite velocity at the leading edge. We discuss the determination of the unknown quantities in the next section.

3. Solution procedure

Our numerical treatment of the problem described in section 2 differs in most respects from that used to derive the results of [4], and not least in our treatment of the integral, in (2.13), of the source distribution along the imaginary axis of the transformed plane. It will be recalled from the discussion in section 1 that the results of Smith [4] are open to criticism as the incidence parameter a becomes small. Thus it might be expected that as $a \to 0$ the vortex system collapses into the leading edge of the wing, and indeed calculations based upon the isolated vortex model of Brown and Michael [11] by Clark, Smith and Thompson [7] support this view. In [4] the source-integral of (2.13) is discretized by a Gaussian formulation, which implies that the continuous distribution of sources is replaced by a distribution of point sources, one at each of

the integration points. It is when the distance of the isolated vortex at Z_V from the wing surface becomes comparable with the spacing of the point sources that the solutions appear to become unsatisfactory. That this is the source of the problem has been demonstrated by the present author [8] who shows that as the source density increases then the isolated vortex approaches closer to the leading edge before the anomalous behaviour observed by Smith [4] manifests itself. In the present work our analytic treatment of the source-integral overcomes this difficulty. It owes its origins to an Appendix of [4], and is specifically appropriate for small values of the incidence parameter a.

Following Barsby [5] we use the intrinsic co-ordinates (σ^*, ψ^*) of Fig. 3 to represent the vortex sheet in the transformed plane. Thus in that plane we have

$$Z^*(\sigma^*) = \int_0^{\sigma^*} e^{i\psi^*(t)}\, dt, \tag{3.1}$$

where we have used $Z^*(0) = 0$. In order to perform the necessary numerical integrations around the vortex sheet we divide it into $2n$ equal steps, of length h, in the arc length σ^*, and so define $2n + 1$ pivotal points in terms of the values of ψ^* at these points. The length of the sheet adopted is determined by the values of h and n. Midway between each pivotal point we have an intermediate point (see Fig. 3). The values of the quantities under consideration at the intermediate points are denoted by a tilde, and it is at these points that we determine the $4n$ unknowns $\tilde{\psi}_i^*$, $\tilde{g}_i^*$, $i = 1, 2, \ldots 2n$. The coordinates of the points on the vortex sheet in the transformed plane are obtained by integrating (3.1) using Simpson's Rule on both the intermediate and pivotal points. The corresponding points in the cross-flow plane can be obtained by integrating (2.10) around the vortex sheet, again using Simpson's Rule. Finally integration along the cut from the last pivotal point Z_{2n+1}^* to the isolated vortex Z_V^* gives the position of the isolated vortex Z_V in the cross-flow plane.

Smith [4] showed that the direction of flow at the leading edge is parallel to the lower surface. Thus with $Z^* = re^{i\theta}$ we determine the value of ψ^* at $Z^* = 0$ from (2.10), and noting that

$$\lim_{r\to 0} \int_0^{re^{i\theta}} \left(\frac{t^2}{t^2 + d^2}\right)^{\epsilon} dt = \frac{r^{1+2\epsilon}\, e^{i\theta(1+2\epsilon)}}{d^{2\epsilon}\,(1+2\epsilon)}, \tag{3.2}$$

so that $\pi(\frac{1}{2} - \epsilon) = \frac{1}{2}\delta = \theta(1 + 2\epsilon)$ at the leading edge, or

$$\psi_1^* = \frac{\pi(\frac{1}{2} - \epsilon)}{1 + 2\epsilon}. \tag{3.3}$$

The remaining values of ψ^* at the pivotal points are obtained by four-point Lagrangian interpolation when the values at the intermediate points $\tilde{\psi}_i^*$ have been determined. For further details of this and subsequent manipulations reference may be made to [8].

At the intermediate points we also have the $2n$ unknown values of the sheet strength $\tilde{g}_i^*$. Now we note that

$$g(\sigma) = -\frac{d\Delta\phi}{d\sigma} = -\frac{d\Delta\phi}{d\sigma^*}\frac{d\sigma^*}{d\sigma} = g^*(\sigma^*)\left|\frac{dZ^*}{dZ}\right| \tag{3.4}$$

which, using (2.10), gives

$$g^*(\sigma^*) = g(\sigma) \left| \left(\frac{Z^{*2}}{Z^{*2}+d^2} \right)^{\epsilon} \right| ,$$

implying that, for finite sheet strength at the physical leading edge $g^*(0) = g_1^* = 0$. The values of g_i^* at the other pivotal points are determined from the values $\tilde{g}_i^*$, again by Lagrangian interpolation.

The remaining three quantities to be determined are the position of the isolated vortex in the transformed plane Z_V^*, and its strength Γ. In all this gives us a total of $4n + 3$ unknown quantities.

We now consider a suitable discretization of the boundary conditions from which we have $4n + 3$ conditions corresponding to our $4n + 3$ unknown quantities.

From the requirement of zero total force on the isolated vortex and cut (2.9), which provides two of the conditions, we have, using (2.13),

$$2\bar{Z}_V - \bar{Z}_E = \left\{ \left(-ia + \frac{S_V}{2\pi i} + R_V \right) \frac{dZ^*}{dZ} \right\}_{Z_V} +$$

$$+ \frac{\Gamma}{2\pi i} \lim_{Z \to Z_V} \left\{ \left(\frac{1}{Z^* - Z_V^*} - \frac{1}{Z^* + \bar{Z}_V^*} \right) \frac{dZ^*}{dZ} - \frac{1}{Z - Z_V} \right\} , \tag{3.5}$$

where we have written

$$S_V = \int_0^{\sigma^*_{\max}} \frac{2g^*(\sigma^*)\, \mathrm{Re}(Z^*(\sigma^*))\, d\sigma^*}{\{Z_V^* - Z^*(\sigma^*)\}\{Z_V^* + \bar{Z}^*(\sigma^*)\}} ,$$

$$R_V = \frac{\cos \epsilon\pi}{\pi i} \int_{-id}^{id} \left| \left(\frac{t^2}{t^2 + d^2} \right)^{\epsilon} \right| \frac{dt}{Z_V^* - t} . \tag{3.6}$$

Now, since

$$\lim_{Z \to Z_V} \left(\frac{1}{Z^* - Z_V^*} \frac{dZ^*}{dZ} - \frac{1}{Z - Z_V} \right) = \frac{1}{2} \left(\frac{d^2 Z^*}{dZ^2} \Big/ \frac{dZ^*}{dZ} \right)_{Z_V} ,$$

using the Taylor series for $Z^* - Z_V^*$, and since from (2.10) we may deduce that

$$\frac{d^2 Z^*}{dZ^2} = - \frac{2\epsilon d^2}{Z^*(d^2 + Z^{*2})} \left(\frac{dZ^*}{dZ} \right)^2 ,$$

the second term on the right-hand side of (3.5) may be written as

$$- \frac{\Gamma}{4\pi i} \left(\frac{1}{\mathrm{Re}(Z_V^*)} + \frac{2\epsilon d^2}{Z_V^*(d^2 + Z_V^{*2})} \right) \left(\frac{Z_V^{*2} + d^2}{Z_V^{*2}} \right)^{\epsilon} .$$

The integral which defines S_V in (3.6) is evaluated by Simpson's Rule which leaves only the

evaluation of R_V in (3.6). Smith [4] obtained the value of this integral numerically, thereby replacing the continuous source distribution by a discrete distribution; however he demonstrated in an Appendix to his paper that R_V could be represented analytically as

$$R_V = \left(\frac{Z_V^{*2}}{Z_V^{*2} + d^2} \right)^{\epsilon} \left\{ 1 - B(\tfrac{1}{2} + \epsilon, 1 - \epsilon) \frac{\cos \epsilon\pi}{\pi(1 - 2\epsilon)} \left(\frac{Z_V^*}{d} \right)^{1-2\epsilon} \times \right.$$
$$\left. \times \, {}_2F_1 \left(1 - \epsilon, \tfrac{1}{2} - \epsilon; \tfrac{3}{2} - \epsilon; -\frac{Z_V^{*2}}{d^2}\right) \right\} , \tag{3.7}$$

where B is the beta function and ${}_2F_1$ the hypergeometric function. Now the series for the hypergeometric function will converge provided $|Z_V^*| < d$. The quantity $d = d(\epsilon)$ may be determined by evaluating (2.10) at the point A of Fig. 2 for which $Z^* = id$. Thus Smith [4] has shown that d^{-1} varies, almost linearly, from 0 to 1.0 as ϵ increases from 0 to 0.5. It is precisely the situation $|Z_V^*/d|$ small which is of interest to us here since for the small values of the incidence parameter a under consideration $|Z_V^*|$ will be small as the vortex configuration collapses into the leading edge. We have therefore evaluated R_V by summing the series for ${}_2F_1$ in (3.7), and in all cases we have terminated the series, whose first term is unity, when the last term is less than 10^{-5} in absolute value.

We have next the Kutta condition of finite velocity at the leading edge which in the transformed plane becomes

$$\frac{dW}{dZ^*} = 0 \quad \text{at} \quad Z^* = 0. \tag{3.8}$$

From (2.13) this may be written, after a little manipulation, as

$$\int_0^{\sigma^*_{\max}} g^*(\sigma^*) \frac{\mathrm{Re}\,(Z^*(\sigma^*))}{|Z^*(\sigma^*)|^2} \, d\sigma^* + \frac{\mathrm{Re}\,(Z_V^*)}{|Z_V^*|^2} \Gamma = \pi a, \tag{3.9}$$

and the integral evaluated using Simpson's Rule.

We now have, in equations (3.5) and (3.9), three conditions with the remaining $4n$ which are required to be determined by applying each of the vortex-sheet conditions (2.6), (2.7) at the $2n$ intermediate points. First we combine (2.6) and (2.7) to give, after a slight re-arrangement

$$\Delta\phi = \Delta\phi_\sigma \{ re^{i\varphi} - (\phi_{\sigma_m} - i\phi_n) \}. \tag{3.10}$$

Now it can be shown [1] that

$$\frac{dW}{d\sigma} = \phi_{\sigma_m} - i\phi_n, \tag{3.11}$$

and from (2.14) we have, following an integration,

$$\Delta\phi = \Gamma + \int_{\sigma^*}^{\sigma^*_{\max}} g^*(t)\, dt. \tag{3.12}$$

Also, with $r = (Z\bar{Z})^{\frac{1}{2}}$, and $\varphi = \psi - \theta$ as in Fig. 2, we may write

$$re^{i\varphi} = \bar{Z}e^{i\psi}, \tag{3.13}$$

and we have

$$\frac{dW}{d\sigma} = \frac{dZ^*}{d\sigma^*}\frac{dW}{dZ^*}\frac{d\sigma^*}{d\sigma} = e^{i\psi^*}\frac{dW}{dZ^*}\left|\frac{dZ^*}{dZ}\right|, \tag{3.14}$$

and so from equations (3.4) and (3.11) to (3.14), the sheet condition (3.10) may be written as

$$\Gamma + \int_{\sigma^*}^{\sigma^*_{\max}} g^*(t)\,dt = -g^*(\sigma^*)e^{i\psi^*}\left|\frac{dZ^*}{dZ}\right|^2\left(\bar{Z}\frac{dZ}{dZ^*} - \frac{dW}{dZ^*}\right), \tag{3.15}$$

which is to be evaluated at each intermediate point $\tilde{Z}_i^*$. The integral on the left-hand side is evaluated using Simpson's Rule. For the right-hand side we note, from (2.13), that

$$\left.\frac{dW}{dZ^*}\right|_{\tilde{Z}_i^*} = -ia + \frac{\Gamma}{2\pi i}\left(\frac{1}{\tilde{Z}_i^* - Z_V^*} - \frac{1}{\tilde{Z}_i^* + \bar{Z}_V^*}\right) + R_i + \frac{S_i}{2\pi i},$$

where R_i is as in (3.7) but with Z_V^* replaced by $\tilde{Z}_i^*$, and is evaluated by again expressing the hypergeometric function as a series, and

$$S_i = \int_0^{\sigma^*_{\max}} g^*(\sigma^*)\left(\frac{1}{\tilde{Z}_i^* - Z^*(\sigma^*)} - \frac{1}{\tilde{Z}_i^* + \bar{Z}^*(\sigma^*)}\right)d\sigma^*. \tag{3.16}$$

We see from (3.16) that we are now required to evaluate a Cauchy Principal-Value integral and as a consequence, following Barsby [5], we rearrange the integrand so that the singularity appears in an integral which can be evaluated analytically. Thus

$$S_i = -\int_0^{\sigma^*_{\max}}\left\{\frac{2g^*(\sigma^*)\,\mathrm{Re}\,(Z^*(\sigma^*))}{\bar{Z}^*(\sigma^*) + \tilde{Z}_i^*} - \frac{g_i^*\,dZ^*/d\sigma^*}{dZ^*/d\sigma^*\,|_{\tilde{Z}_i^*}}\right\}\frac{d\sigma^*}{Z^*(\sigma^*) - \tilde{Z}_i^*}$$
$$- \tilde{g}_i^*\,e^{-i\tilde{\psi}_i^*}\ln\left(\frac{Z_{2n+1}^* - \tilde{Z}_i^*}{\tilde{Z}_i^* - Z_i^*}\right). \tag{3.17}$$

We now have, from (3.5), (3.9) and (3.15) a total of $4n + 3$ nonlinear algebraic equations for the $4n + 3$ unknown quantities $\tilde{\psi}_i^*, \tilde{g}_i^*$ $(i = 1, 2, \ldots 2n)$, Z_V^* and Γ. To solve these equations we do not use the nested iteration scheme of Smith [1], [4] but the more direct Newton iteration method employed by Barsby [3], [5]. Thus we write the equations in the form

$$f_i(\mathbf{x}) = 0, \quad i = 1, 2, \ldots 4n + 3,$$

where $\mathbf{x}$ is the vector of the $4n + 3$ unknowns, and then use the iterative solution procedure

$$\mathbf{x}^{k+1} = \mathbf{x}^k - (J^k)^{-1}\,\mathbf{f}^k,$$

where a superscript k denotes the k^{th} iteration and J^k is the Jacobian matrix $\partial f_i^k/\partial x_j$. This iterative procedure gives quadratic convergence, but in practice to obtain a solution we find it necessary to invert the matrix only once (or at most twice) and so effectively only gain linear convergence. For the solutions presented below the iterative scheme was deemed to have converged when

$$\left(\sum_{i=1}^{4n+3} f_i^2\right)^{\frac{1}{2}} < 10^{-6}. \tag{3.18}$$

Given a solution at a particular point (a, ϵ) in parameter space then to obtain a new solution we have usually fixed one of these parameters and varied the other by about 10%. With the original solution as the zeroth iterate we have found that convergence to a new solution, as defined by (3.18), is usually obtained within about 10 iterations.

The results we have obtained in the manner outlined in this section are described below.

4. Results

Before describing the results obtained by the method set out in section 3 we note that the total circulation about the vortex configuration is given simply as

$$\Gamma_t = \Gamma + \int_0^{\sigma^*_{\max}} g^*(\sigma^*)\,\mathrm{d}\sigma^* \tag{4.1}$$

and we have evaluated the integral in (4.1) using Simpson's rule in which both the pivotal and intermediate points are employed.

The length of the vortex sheet used in the calculations is determined by the number $2n$, and spacing h, of the pivotal points. In all our calculations the angular extent of the sheet was maintained approximately constant by taking $n = 6$ and $h = \frac{1}{8}\,|Z_V^*|$. As Smith [1] has demonstrated, there is virtually no advantage to be gained from the use of longer sheets.

Results have been obtained in (a, ϵ)-space by fixing one parameter and varying the other. Initially we have compared our results for $\epsilon = 0.5$ and various values of the incidence parameter a with the results for the flat-plate delta wing in [1], [3], and also for $a = 1.0$ and various values of the thickness parameter ϵ with the results of [4] for a thick wing. Agreement was found for the position of the isolated vortex and overall circulation to within less than 3%. This was considered acceptable in view of the differences between the various methods used to derive the solutions.

As we have noted in earlier sections there is an apparent difficulty with the results of Smith [4] in that as the incidence parameter a decreases the vortex configuration, and in particular the isolated vortex core, does not collapse as expected into the leading edge. We discuss that aspect of our solutions first with reference to Figs 4 to 6. Consider Fig. 5 where the thickness parameter $\epsilon = \frac{1}{6}$ which is the value for which Smith's solutions are apparently least satisfactory. We show the position of the isolated vortex for this wing as the incidence parameter is reduced to zero and consider first Smith's results. The solutions terminate at $a = 0.2$ and it can be seen that for $a = 0.3$, 0.2 the vortex is moving towards the wing surface rather than the leading edge. In

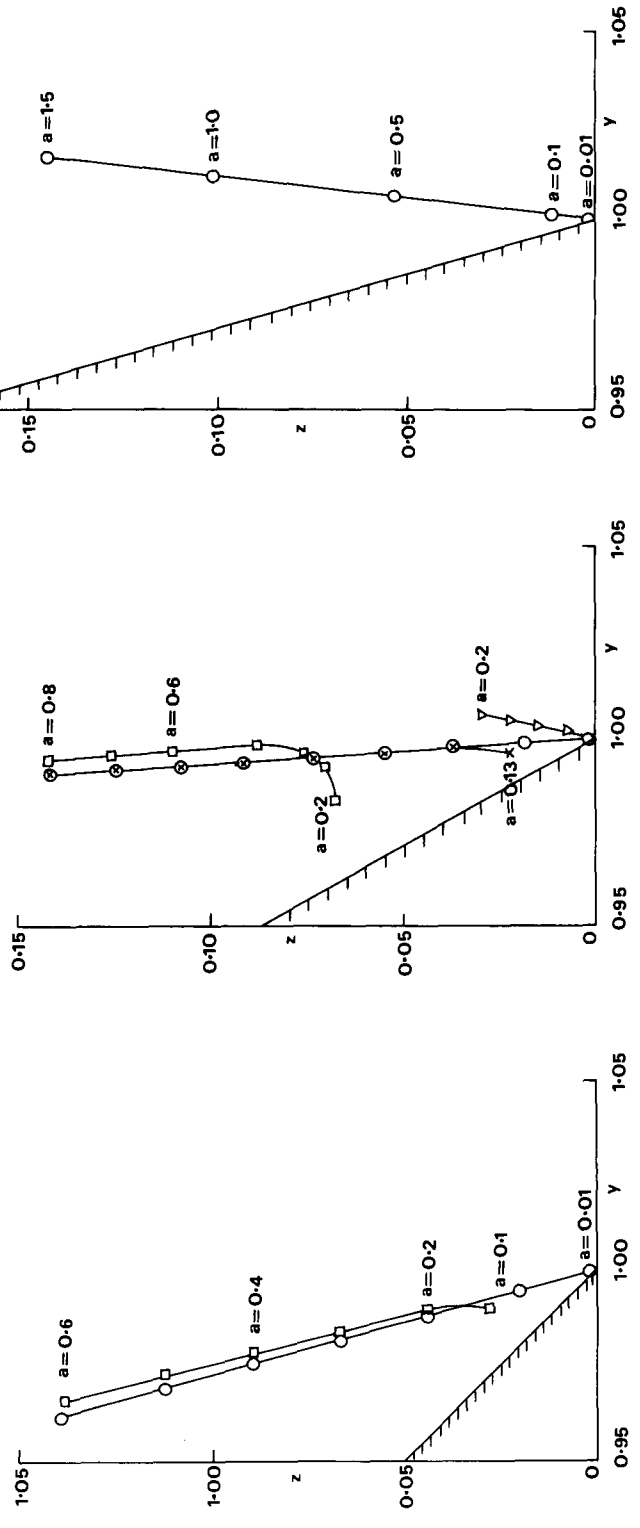

Figure 6. Variation of vortex position with the incidence parameter a for $\epsilon = \frac{1}{12}$, $\delta = 150°$ using the present method.

Figure 5. Variation of vortex position with the incidence parameter a for $\epsilon = \frac{1}{6}$, $\delta = 120°$. The results of Smith [4] are shown as —□—, the results from a 500-point discretisation as —×—, the present results as —○—, and the results of Clark, Smith and Thompson [7] as —▽—.

Figure 4. Variation of vortex position with the incidence parameter a for $\epsilon = \frac{1}{4}$, $\delta = 90°$. The results of Smith [4] are shown as —□—, and the present results as —○—.

deriving his results Smith uses an integration formula which effectively replaces the continuous source distribution by 50 discrete sources. We have repeated his calculations with 500 discrete sources and these are seen to be satisfactory for $a > 0.2$ but again become unsatisfactory as a decreases below that value. Clearly for any fixed value of a the solution can be made satisfactory by increasing the number of discrete sources, but such a process is prohibitive in terms of computer time. By treating the source-integral analytically, and evaluating the hypergeometric function from its series expansion as described in section 3, we are able to find solutions much more economically, and as seen in Figs 4 to 6 we are able to obtain solutions at very small values of a. The solutions obtained in this way have no unsatisfactory features, and the vortex centre is seen to move almost linearly into the leading edge. Also in Fig. 5 are shown results obtained in [7] using an isolated vortex model. Again as $a \to 0$ the vortex moves to the leading edge, but as incidence increases these results are seen to be inadequate. In Figs 4 and 6 we show the results of our present calculations for $\epsilon = \frac{1}{4}, \frac{1}{12}$, respectively and, where available, compare with the results in [4].

For the case of a flat-plate delta wing, for which $\epsilon = 0.5$, Barsby [3] found that for $a \leqslant 0.038$ the vortex sheet no longer separated from the leading edge, but from a point on the wing surface just inboard of the edge. For the case of the thick wing with $\epsilon = \frac{1}{6}$ we found that the incidence parameter could be reduced to $a = 10^{-5}$ with no evidence of inboard separation. To discover at what value of ϵ separation first moves inboard from the leading edge a sequence of results for $a = 0.01$ with increasing ϵ was obtained. No solutions could be found for $\epsilon > 0.392$, and since our model is not appropriate for inboard separation we presume that the separation point moves inboard

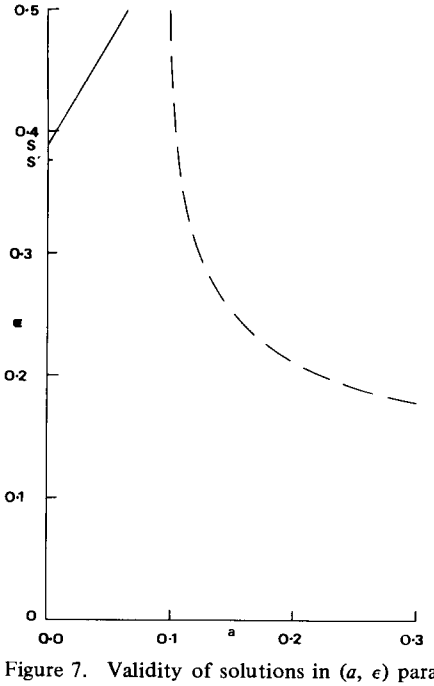

Figure 7. Validity of solutions in (a, ϵ) parameter space. Smith's [4] solutions are valid to the right of the broken line, whilst satisfactory solutions have been obtained by the present method to the right of the full line. Inboard solutions only are available to the left of that line. The points S, S' correspond to leading-edge angles of 39.5° and 42.5° respectively.

at this value. From further investigation we were able to delineate a relatively small area in (a, ϵ)-space in which no solution with leading-edge separation exists. This is shown in Fig. 7 and it seems reasonable to assume that inboard separation occurs here, contrary to the conjecture in [3] that inboard separation is the result of a lack of thickness of the wing. Extrapolation in Fig. 7 to the point S shows that for wings of leading-edge angle less than about 39.5° inboard separation will be obtained for sufficiently small values of a. The corresponding value from the isolated vortex model described in [7] is 42.5°. Also shown in Fig. 7 is the approximate limit of validity of Smith's solutions [4]. The criterion for validity is that the distance between the isolated vortex of Smith's solutions and that in the present solutions must be less than one tenth of the distance between the leading edge of the wing and the isolated vortex.

In Fig. 8 we give a typical example of the effect of wing thickness on the shape of the vortex sheet and position of the vortex core. Thus as the thickness increases there is a marked movement of the vortex core outboard and a shrinkage of the whole vortex system towards the lead-

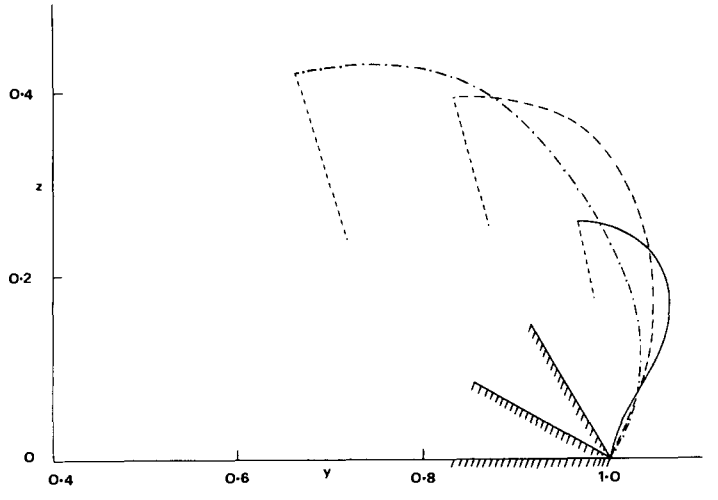

Figure 8. Sheet shapes and vortex positions for $a = 1.0$. $\epsilon = \frac{1}{6}$, ——— ; $\epsilon = \frac{1}{3}$, – – – – ; $\epsilon = \frac{1}{2}$, —·—·—·—.

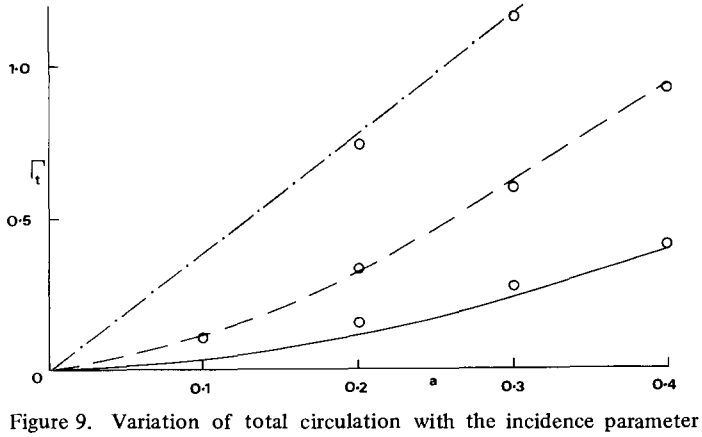

Figure 9. Variation of total circulation with the incidence parameter a. $\epsilon = \frac{1}{6}$, ——— ; $\epsilon = \frac{1}{3}$, – – – –, $\epsilon = \frac{1}{2}$, —·—·—·—·—. The results obtained by Smith [4] are shown thus ○.

ing edge. The point of inflexion on the sheet for the thickest wing shown in Fig. 8 is associated with the fact that the vortex sheet leaves the leading edge in a direction tangential to the lower surface.

The variation of total circulation, calculated from (4.1), with the incidence parameter a for wings of three different thicknesses is shown in Fig. 9. We note that the initial rate of growth of circulation at zero incidence is zero for thick wings although for the case of the flat plate, $\epsilon = \frac{1}{2}$, it is non-zero. This agrees with the results for the simpler model of [7]. Also shown in Fig. 9 are the results of Smith [4]; as for the vortex position differences between those results and the results obtained by the present method are apparent. Finally we note that it was observed during the course of the present calculations that the proportion of circulation on the finite vortex sheet decreases as the wing thickness increases.

Acknowledgements

The author is indebted to Professor N. Riley, University of East Anglia and Mr J. H. B. Smith, RAE, Farnborough for helpful discussions and guidance. During the period in which this work was carried out the author was in receipt of a Science Research Council Studentship.

REFERENCES

[1] J. H. B. Smith, Improved calculations of leading-edge separation from slender delta wings, *Proc. R. Soc.* A306 (1968) 67-90.
[2] J. E. Barsby, Calculations of the effect of blowing from the leading edges of a slender delta wing, *ARC R. & M. No. 3692 (1972) 74 pp.*
[3] J. E. Barsby, Separated flow past a slender delta wing at incidence, *Aero. Quart.* 24 (1973) 120-128.
[4] J. H. B. Smith, Calculations of the flow over thick, conical, slender wings with leading-edge separation, *RAE TR 71057 (1971) 59 pp.*
[5] J. E. Barsby, Calculations of the effects of blowing from the leading edges of a cambered delta wing, *ARC R. & M. No. 3800 (1978) 51 pp.*
[6] G. N. Ward, *Linearised theory of steady high-speed flow*, Cambridge University Press, 1955.
[7] R. W. Clark, J. H. B. Smith and C. W. Thompson, Some series-expansion solutions for slender wings with leading-edge separation, *ARC R. & M. No. 3785 (1976) 56 pp.*
[8] J. Nutter, *Ph. D. Thesis*, University of East Anglia (1979).
[9] D. L. I. Kirkpatrick, Investigation of the normal force characteristics of slender delta wings with various rhombic cross-sections in subsonic conical flow, *RAE TR 65291 (1965) 53 pp.*
[10] P. T. Fink and J. Taylor, Some early experiments on vortex separation, *ARC R. & M. 3489 (1967) 47 pp.*
[11] C. E. Brown and W. H. Michael, Effect of leading-edge separation on the lift of a delta wing, *J. Aero. Sci.* 21 (1954) 690-694.